Manuscript was accepted fo publication to Eur. J. Inorg. Chem. 2016, 3530–3535
Published version: http://onlinelibrary.wiley.com/doi/10.1002/ejic.201600606

SHORT COMMUNICATION

Multi-readout logic gate for selective metal ions detection in parts per billion levels

Nadia O. Laschuk,[a] Iraklii I. Ebralidze,[a] Denis Spasyuk,[b][‡] and Olena V. Zenkina*[a]

Abstract: Optical sensors utilizing visual responses for metal ions identification require reliable molecular systems able to selectively operate in multicomponent solutions. Herein we report water soluble terpyridyl based ligand that demonstrates effective quantification of ppb to ppm levels of Fe^{2+}, Fe^{3+}, Zn^{2+}, and Ru^{3+}. While Fe^{3+} and Ru^{3+} ions bind to the ligand to form monometallic complex, 2:1 ligand to metal binding stoichiometry was found for Zn^{2+} and Fe^{2+} complexes. Corresponding metal binding events are directly translated into distinct colorimetric and spectroscopic logic outputs. Applying molecular logic (Boolean logic operations) to describe these binding events, selective discrimination between the ions was demonstrated.

Introduction

Transition metals play a vital role in biology and chemistry. Among the various transition metals, iron is the most abundant essential trace element in the human body, which plays crucial roles in physiological processes such as oxygen transport, electron transfer, and enzymatic catalysis.[1] Iron deficiency may lead to anemia, organ dysfunction, and tumorigenesis. Paradoxically, too much iron is equally hazardous to health due to its ability to generate free radicals that increase risk of cancer[2] and Alzheimer Disease.[3] Zinc is the second most abundant transition metal in human body after iron.[4] Unlike iron, which is required for certain specific functions, zinc is required for general metabolism.[5] However, increased dietary zinc exhibits significant memory deficits and may cause Alzheimer's disease,[6] a failure of zinc homeostasis is linked to development of prostate cancer,[7] and finally, accumulation of zinc to toxic levels leads to cell death.[8]

Extensive use of ruthenium catalysts in industrial processes, generation of e-wastes where Ru is employed as a hardener in Pt/Ru alloys, and use of ruthenium in medicine[9] result in raising of ruthenium content in the environment.[10] Recent success in development of water splitting process catalyzed by ruthenium complexes may potentially become an additional supply of ruthenium to the environment, since metal leaching is a typical issue for many catalytic processes.[11] Even though ruthenium is not an essential trace element in the human body, it may have significant impact on human health; in particular, ruthenium complexes were shown to form cross-links with nucleic acids to halt DNA replication.[12]

Although significant progress has been made in monitoring of iron(II),[13] iron(III),[14] zinc(II),[15] and ruthenium(III)[16] as single-analyte ions, as well as in detection of iron(II)-iron(III) pair,[17] recent research efforts have been focused on the development of assays that allow simultaneous multi-analyte detection in ppb to ppm level,[17-18] which is especially important in environmental testings, food chemistry and molecular biology.[19]

Since the seminal work by de Silva who invented the first two-input molecular logic gate,[20] many types of logic gates responsive to two physical and/or chemical signals have been successfully demonstrated.[21] Implementation of multianalyte assays in molecular-scale devices resulting in sensor arrays in solution remains challenging.[22] Here we report on development of a water-soluble ligand able to simultaneously detect several metal ions.

Results and Discussion

The ligand 2,2':6',2"-terpyridine (terpy) is known to form complexes with variety of metals.[23] However, low solubility of terpy in water constrains the use of this ligand for direct metal detection in aqueous media. To avoid this problem, we decorated terpy by polar diethylphosphonate group resulting in $terpyPO_3Et_2$, ligand **1** (Scheme 1) as previously described.[24] Being more polar than terpy, **1** is soluble, and can form soluble metal complexes in alcohol-water mixtures. For example solubility of **1** in deionized (DI) water: ethanol mixture (80:20 v/v) was found to be 28 mM. Yet, solubility of **1** in 100% DI water (0.1 mM saturated) remains quite low. Further hydrolysis of **1** in acidic conditions results in $terpyPO_3H_2$, ligand **2**, which is readily soluble in DI water at concentrations up to 66 mM.

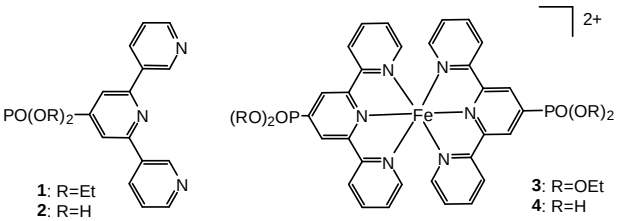

Scheme 1. Ligands $terpyPO_3Et_2$, (**1**), $terpyPO_3H_2$, (**2**) and their Fe^{2+} complexes. $[Fe(terpy\text{-}PO_3H_2)_2]^{2+}$ (**3**) and $[Fe(terpy\text{-}PO_3Et_2)_2]^{2+}$ (**4**).

To probe metal sensing ability in water, UV-vis absorbance and fluorescence emission spectra of **2** (4.7 ppm, 0.015 mM) with various metal cations (15 ppm) were measured. Presence of

[a] Faculty of Science, University of Ontario Institute of Technology, 2000 Simcoe Street North, Oshawa, ON, Canada, L1H 7K4
E-mail: olena.zenkina@uoit.ca
[b] Department of Chemistry, University of Calgary, 2500 University Drive NW, Calgary, AB, Canada, T2N 1N4.
[‡] Current address: Canadian Light Source Inc. 44 Innovation Boulevard Saskatoon, S7N 2V3 SK, Canada

Supporting information for this article is available on the WWW under http://dx.doi.org/10.1002/ejicxxxxxxxxx. CCDC 1427073 can be obtained from The Cambridge Crystallographic Data Centre.

Fe^{2+}, Fe^{3+}, Ru^{3+}, and Zn^{2+} resulted in significant changes of either the absorption or emission spectrum (Figs. 1, S2), but no distinct changes were observed for Al^{3+}, Ba^{2+}, Ca^{2+}, Cs^{+}, Co^{2+}, Cr^{3+}, Cu^{2+}, Ir^{2+}, K^{+}, Li^{+}, Mg^{+}, Mn^{2+}, Na^{+}, Ni^{2+}, Pd^{2+}, and Sn^{2+}. When **2** was mixed with Fe^{2+} ion in water, colourless solutions immediately turned pink (Fig S1) due to the formation of complex **3**. A characteristic metal to ligand charge transfer band is observed at 560 nm (ε_{560}=1.197·10^4 M·cm^{-1}). Presence of Fe^{2+} and Ru^{3+} ions in relatively high concentrations (15 ppm) in limiting (4.7 ppm, 0.015 mM) water solutions of **2** can be tracked by the appearance of characteristic bands at λ_{abs} = 560 nm and λ_{abs} = 400 nm, respectively.

Significant increase in intensity of the absorption λ_{abs} = 290 nm is due to either Ru^{3+} or Fe^{3+}. Comparing the change in intensities of λ_{abs} = 290 nm and λ_{abs} = 400 nm, Ru^{3+} or Fe^{3+} ions can be discriminated. Furthermore, mixtures of **2** with Zn^{2+} show strong fluorescence emission at λ_f = 360 nm and λ_f = 700 nm upon excitation at 326 nm. Thus, by combination of the UV-vis and fluorescence data, it is possible to detect and differentiate between all four metal ions (Fig. 1). To get inside the formation of metal complexes of these four target metal cations with **2** in aqueous media, UV-vis and fluorescence emission spectra of DI water solutions containing excess of **2** and limiting amounts of metal salts were recorded.

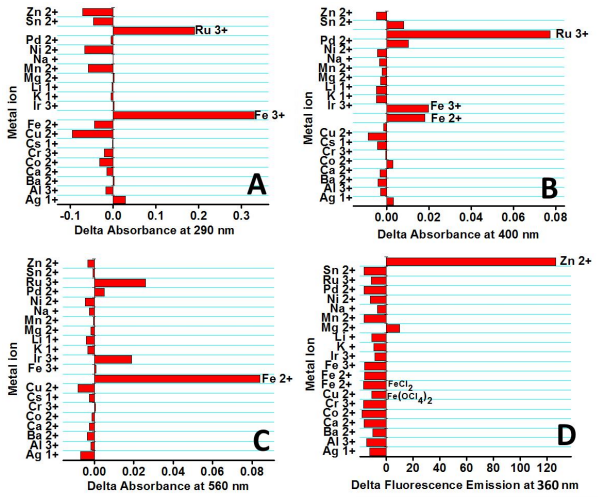

Figure 1. Representative UV-vis absorbance changes upon addition of metal salts (15 ppm) to 2 (4.7 ppm) in DI water: A) at 290 nm; B) at 400 nm; C) at 560 nm. D) Representative fluorescence emission changes upon addition of metal salts (15 ppm) to 2 (4.7 ppm) in DI water at 360 nm.

Using the UV-vis absorbance response at λ_{abs} =560 nm, we could detect as low as 50 ppb of Fe^{2+} in aqueous solutions in presence of 15 ppm of **2**. Increasing Fe^{2+} concentration up to 1000 ppb results in a linear increase of the response (Fig. 2A). Importantly, detection of Fe^{2+} ions was found to be independent on the nature of anion (Cl^- vs ClO_4^-). Identical linear correlations were found for detection of $FeCl_2$ (black line, R^2=0.997) and $Fe(ClO_4)_2$ (red line, R^2=0.997), Fig. 2A. Similar experiments performed with **1** in DI water : ethanol (20%:80% v/v) (Figure 2 B) allow to detect *as low as of 50 ppb of* Fe^{2+} with the linear increase of the response up to 1000 ppb of Fe^{2+}. The similarity of these results suggests that PO_3Et_2 and PO_3H_2 groups in **1** and **2** do not participate in coordination with Fe^{2+}.

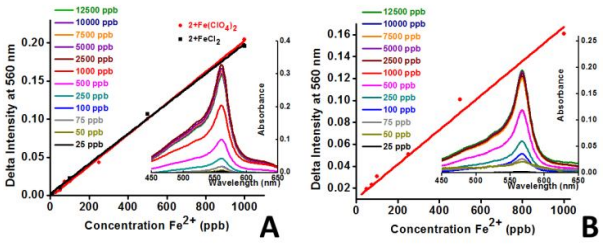

Figure 2. UV-vis absorbance of A) mixed aqueous solution containing **2** (15 ppm, 0.048 mM), and B) water : ethanol solution containing **1** (15 ppm, 0.041 mM), (right) with different concentrations of Fe^{2+}.

Linear increase of absorbance intensities of aqueous solutions of **2** in presence of Fe^{3+} or Ru^{3+} ions up to 1:1 ligand to metal stoichiometric ratio, suggests the formation of a monometallic complex in both cases (Figs. S10, S11). On the contrary, increase of Fe^{2+} concentration in an aqueous solution of **2** results in relatively narrow linear area of the absorbance followed by deviation from linearity and saturation of the signal. This suggests the formation of complexes where more than one ligand (L) per Fe^{2+} (M) ion is involved.

Indeed, HRMS analysis of Fe^{2+} to **2** adduct (complex **3**) gives molar mass that corresponds to L_2M structure (see SI). Moreover, slow evaporation of isopropanol-water mixture containing excess of Fe^{2+} and **1** as a limiting reagent, results in X-Ray quality L_2M crystals of complex **4** (Fig. 3A). The complex displays a slightly distorted octahedral geometry around Fe (II) center formed by coordination of two molecules of ligand **1** via terpyridine moieties situated in almost orthogonal fashion.

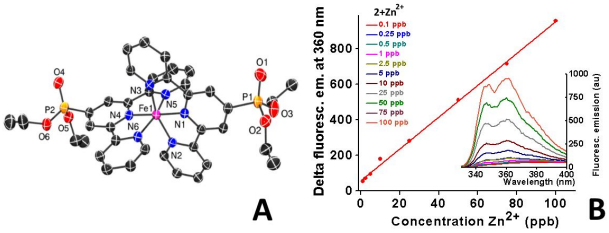

Figure 3. A) Crystallographically determined structure of [Fe(terpy-$PO_3Et_2)_2$]$(ClO_4)_2$ (**4**). Thermal ellipsoids drawn at the 30% confidence level. Hydrogen atoms, counter anions (ClO_4^-) and solvent molecules (H_2O) are omitted for clarity. B) Fluorescence emission at 360 nm of a mixed aqueous solution containing compound **2** (1 ppm, 3.19·10^{-6} M) with different concentrations of Zn^{2+}.

Presence of Zn^{2+} ions in aqueous solutions of **2** can be detected by the appearance of two fluorescence emission bands (λ_f = 360 nm and λ_f = 700 nm). Band at 360 nm has quantum

yield (QY) of 0.75, which is much higher than QY of a common fluorescence standard tryptophan (0.14), and thus can be used to quantify ultra-small concentrations of Zn^{2+} (*as low as 0.25 ppb of* Zn^{2+} can be detected by 1 ppm solution of **2**, Fig 3B). On the contrary, band at 700 nm is lower in intensity and can be used to detect and quantify significantly higher concentrations of Zn^{2+} (Figs. S14). To establish stoichiometry of the coordination of **2** with all four metal ions, continuous variation analysis procedure (Jobs plot) was performed with the corresponding absorbance and fluorescence intensity data (Fig. 4). Examination of the Jobs plot suggests 2:1 ligand (L) to metal (M) binding stoichiometry for Zn^{2+} and Fe^{2+} complexes that is consistent with literature reports for structurally related complexes.[25] Performing titration of **2** by Zn^{2+} as well as by Fe^{2+} in phosphate buffer (pH 7.0) results in similar (within the measurement error) results. Fe^{3+} and Ru^{3+} form 1:1 L:M complex.

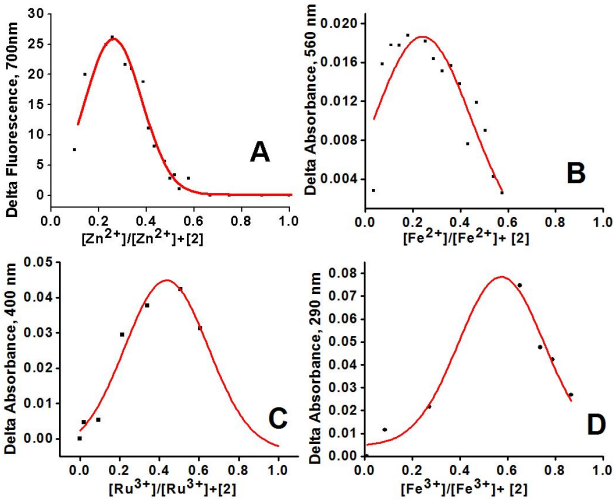

Figure 4. Jobs plot for **2** and A) Zn^{2+} (in phosphate buffer, pH 7.0), B) Fe^{2+} (in phosphate buffer, pH 7.0), C) Ru^{3+}, and D) Fe^{3+}, suggesting the formation of a 2:1 (L:M) complex in cases of Zn^{2+} and Fe^{2+}; and 1:1 (L:M) complex in cases of Ru^{3+} and Fe^{3+}.

To discover ability of **2** for simultaneous detection of few metal cations, absorbance and fluorescence of **2** (excess, 15 ppm) in presence of target cation and competing metal ion or mixtures of few metal ions (1 ppm each) were studied. When Fe^{2+} is present in the solution, intensity of the characteristic absorbance band at 560 nm is almost not affected by the presence of Zn^{2+}, Ru^{2+}, and Fe^{3+} in different combinations (Fig 5). To probe if our system is applicable to real objects, samples of apple juice (Rougemont) and apple cider (Wellesley) were analyzed. The amount of Fe^{2+} determined by $\Delta\lambda_{abs}$ = 560 nm using standard addition method in juice (0.0210 mM) and cider (0.0321 mM) is consistent with the results of total iron determined by atomic absorption spectroscopy (0.0242 mM and 0.0344 mM, respectively). The same (within experimental ettor) results were obtained when the samples were treated with hydroxylamine that is known to reduce Fe^{3+} to Fe^{2+} thus suggesting that most of the iron in both solutions consists in Fe^{2+} form and confirming the statement.

However, the intensity of both fluorescence emission maxima at 360 nm and 700 nm of water solutions of Zn^{2+} (1 ppm) and **2** (15 ppm, 0.048 mM) decrease significantly (yet does not quench completely) in presence of 1 ppm of Fe^{2+} (Fig. 5). Moreover, presence of Fe^{2+}, Fe^{3+}, Ru^{3+}, and Zn^{2+} ions (1 ppm each) in water solutions containing an excess of ligand (15 ppm), results in a complex optical and fluorescence response that can be analyzed utilizing molecular logic gates concept.

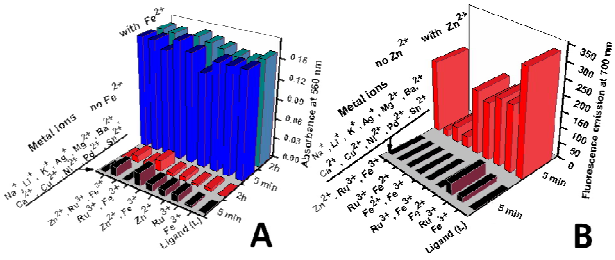

Figure 5. Uv-vis absorbance intensity at 560 nm (A) and fluorescence emission at 700 nm (B) responses of **2** (15 ppm in water, 0.048 mM) to various metal ions. Black bars represent the absorption of **2** in the presence of selected metal ion(s) (1 ppm each) without Fe^{2+} (A) and without Zn^{2+} (B) after 5 min, respectively. Blue and green bars represent the absorption of **2** at 560 nm in presence of Fe^{2+} and a competitive ion or a mixture of competitive metal ions (1 ppm each) after 5 min and 2 h, respectively. Red bars represent the absorption of **2** at 700 nm (excitation on 326 nm) in presence of Zn^{2+} (1 ppm) and a competitive ion or a mixture of competitive metal ions (1 ppm each) after 5 min.

In the following set of experiments, four chemical inputs Fe^{2+}, Ru^{3+}, Fe^{3+}, and Zn^{2+} were used to address the optical outputs of the λ_{abs} = 516 nm λ_{abs} = 400 nm, λ_{abs} = 290 nm, and the change in fluorescence emission intensity λ_{f1} = 360 nm (Table S1). For designing logic gates, addition of 1 ppm of the corresponding metal salt to 15 ppm of aqueous solution of **2** was considered as Input = 1, else Input = 0. Similarly, the significant optical changes observed (Δ) were considered as Output = 1, else Output = 0. As expected, presence of Fe^{2+} (1 ppm) in water solution of **2** (15 ppm, 0.048 mM) results in increase of absorbance intensity at λ_{abs} = 560 nm (output A). The output A = 1 level (here $\Delta_{560} \geq 0.1$ a.u.) is not affected by presence of Fe^{3+}, Ru^{3+}, Zn^{2+}, or their mixtures.

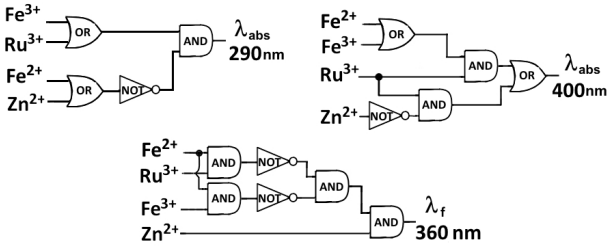

Figure 6. Logic circuit for the 4-input and 4-output logic gate system. Each output is separated for clarity. Since output λabs = 560 nm depends only on presence of Fe^{2+}, the logic circuit is not shown.

The response at 400 nm (output B) is positive (here $\Delta_{400} \geq 0.012$ a.u.) in presence of Ru^{3+} (trial 3). Presence of Zn^{2+} together with Ru^{3+} results in the signal disappearance, i.e output B = 0 (trial 10). Thus using Zn^{2+} ions as an input, NOT gate was implemented followed by AND gate joining Zn^{2+} and Ru^{3+} inputs and resulting in an INHIBIT logic gate. On the other hand, mixture of Ru^{3+} with either Fe^{2+} OR Fe^{3+} (trials 6 and 9, respectively) as well as mixture of Ru^{3+} with both Fe^{2+} AND Fe^{3+} (trial 12), and even Ru^{3+} with Fe^{2+}, Fe^{3+}, and Zn^{2+} (trial 16) result in a positive (output B = 1) response. Presence of Zn^{2+} together with either Fe^{2+} (trial 8) or Fe^{3+} (trial 11) result in insignificant optical response (output B = 0, $\Delta_{400} < 0.012$ a.u.). Output at 290 nm is positive (Output C = 1, $\Delta_{290} \geq 0.17$ au) when Fe^{3+} and/or Ru^{3+} is/are present in the system (trials 3, 4, and 9). Presence of either Fe^{2+} or Zn^{2+} or both Fe^{2+} AND Zn^{2+} inhibits output C. Fluorescence emission output at 360 nm is positive (Output D=1, if $\Delta_{f360} \geq 2000$ au) in presence of Zn^{2+} (trial 5). However, presence of Fe^{2+} AND at least one of the other ions (Fe^{3+} or Ru^{3+}) INHIBITs fluorescence.

Conclusions

In summary, we have developed a promising sensing platform for rapid and sensitive detection of Fe^{2+}, Fe^{3+}, Ru^{3+}, and Zn^{2+} in aqueous solutions, which is potentially applicable for analysis of environmental, food, biological and biomedical systems. Unique responses from these four metal cations could be detected by the combination of UV-vis and fluorescence spectroscopy. To get fundamental understanding of this sensing system, metal–ligand stoichiometries were studied. Corresponding metal binding events are directly translated into distinct colorimetric and spectroscopic logic outputs. By utilizing all acquired knowledge we were able to apply molecular logic (Boolean logic operations) to describe the interaction between the ligand (as a logic gate) and four target cations (four logical inputs). We believe that the combination of these logic gates with other novel technologies, such as 'lab-on-a-chip' and even 'lab-on-a-molecule', could bring about a broad range of applications in analytical and material sciences.

Acknowledgements

Research supported by the University of Ontario Institute of Technology start-up grant and NSERC Discovery grant.

Keywords: Metal-ligand recognition • sensors • molecular logic • X-ray • terpy

[1] a) O. Han, *Metallomics* **2011**, *3*, 103-109; b) D. J. A. Netz, M. Stuempfig, C. Dore, U. Muehlenhoff, A. J. Pierik, R. Lill, *Nat. Chem. Biol.* **2010**, *6*, 758-765.

[2] C. P. Wen, J. H. Lee, Y.-P. Tai, C. Wen, S. B. Wu, M. K. Tsai, D. P. H. Hsieh, H.-C. Chiang, C. A. Hsiung, C. Y. Hsu, X. Wu, *Cancer Res.* **2014**, *74*, 6589-6597.

[3] G. M. Bishop, S. R. Robinson, Q. Liu, G. Perry, C. S. Atwood, M. A. Smith, *Dev. Neurosci.* **2002**, *24*, 184-187.

[4] A. S. Prasad, *Ann. Intern. Med.* **1996**, *125*, 142-143.

[5] J. C. King, *Am. J. Clin. Nutr.* **2011**, *94*, 679S-684S.

[6] J. M. Flinn, P. L. Bozzelli, P. A. Adlard, A. M. Railey, *Front. Aging Neurosci.* **2014**, *6*.

[7] L. C. Costello, R. B. Franklin, *Mol. Cancer* **2006**, *5*, 17.

[8] G. J. Fosmire, *Am. J. Clin. Nutr.* **1990**, *51*, 225-227.

[9] a) B. A. Albani, B. Peña, N. A. Leed, N. A. B. G. de Paula, C. Pavani, M. S. Baptista, K. R. Dunbar, C. Turro, *J. Am. Chem. Soc.* **2014**, *136*, 17095-17101; b) B. Peña, A. David, C. Pavani, M. S. Baptista, J.-P. Pellois, C. Turro, K. R. Dunbar, *Organometallics* **2014**, *33*, 1100-1103.

[10] P. Westerhoff, S. Lee, Y. Yang, G. W. Gordon, K. Hristovski, R. U. Halden, P. Herckes, *Environ. Sci. Technol.* **2015,** *49*, 9479-9488.

[11] a) C. Luo, S. Wang, H. Liu, *Angew. Chem. Int. Ed* **2007**, *46*, 7636-7639; b) M. A. Hanif, I. I. Ebralidze, J. H. Horton, *Appl. Surf. Sci.*, *280*, 836-844.

[12] A. Bergamo, C. Gaiddon, J. H. M. Schellens, J. H. Beijnen, G. Sava, *J. Inorg. Biochem.* **2012**, *106*, 90-99.

[13] a) P. L. Croot, P. Laan, *Anal. Chim. Acta* **2002**, *466*, 261-273; b) H. Tamura, K. Goto, T. Yotsuyanagi, M. Nagayama, *Talanta* **1974**, *21*, 314-318.

[14] a) C. R. Lohani, J.-M. Kim, K.-H. Lee, *Bioorg. Med. Chem. Lett.* **2009**, *19*, 6069-6073; b) U. Fegade, S. Tayade, G. K. Chaitanya, S. Attarde, A. Kuwar, *J. Fluoresc.* **2014**, *24*, 675-681.

[15] a) J. Peng, W. Xu, C. L. Teoh, S. Han, B. Kim, A. Samanta, J. C. Er, L. Wang, L. Yuan, X. Liu, Y.-T. Chang, *J. Am. Chem. Soc.* **2015**, *137*, 2336-2342; b) J. H. Choi, J. Y. Ryu, Y. J. Park, H. Begum, H.-R. Park, H. J. Cho, Y. Kim, J. Lee, *Inorg. Chem. Commun.* **2014**, *50*, 24-27.

[16] a) T. Suoranta, M. Niemelä, P. Perämäki, *Talanta*, *119*, 425-429; b) E. Zambrzycka, U. Kiedysz, A. Z. Wilczewska, B. Lesniewska, B. Godlewska-Zylkiewicz, *Anal. Methods* **2013**, *5*, 3096-3105.

[17] S. Goodwin, A. M. Gade, M. Byrom, B. Herrera, C. Spears, E. V. Anslyn, A. D. Ellington, *Angew. Chem. Int. Ed.* **2015**, *54*, 6339-6342.

[18] a) L. You, D. Zha, E. V. Anslyn, *Chem. Rev.* **2015**, *115*, 7840-7892; b) Z. Zhang, D. S. Kim, C.-Y. Lin, H. Zhang, A. D. Lammer, V. M. Lynch, I. Popov, O. Š. Miljanić, E. V. Anslyn, J. L. Sessler, *J. Am. Chem. Soc.* **2015**, *137*, 7769-7774.

[19] a) B. Rout, L. Motiei, D. Margulies, *Synlett* **2014**, *25*, 1050-1054; b) L. Motiei, Z. Pode, A. Koganitsky, D. Margulies, *Angew. Chem. Int. Ed* **2014**, *53*, 9289-9293.

[20] A. P. de Silva, H. Q. N. Gunaratne, C. P. McCoy, *Nature* **1993**, *364*, 42-44.

[21] a) T. Gupta, M. E. van der Boom, *Angew. Chem., Int. Ed.* **2008**, *47*, 5322-5326; b) G. de Ruiter, M. E. van der Boom, *Angew. Chem. Int. Ed* **2012**, *51*, 8598-8601; c) D. Margulies, A. D. Hamilton, *J. Am. Chem. Soc.* **2009**, *131*, 9142-9143; d) S. Sahu, T. B. Sil, M. Das, G. Krishnamoorthy, *Analyst* **2015**, *140*, 6114-6123; e) T. J. Farrugia, D. C. Magri, *New J. Chem* **2013**, *37*, 148-151.

[22] K. Chen, Q. Shu, M. Schmittel, *Chem. Soc. Rev.* **2015**, *44*, 136-160.

[23] Constable E.C, *The Coordination Chemistry of 2,2′:6′,2″-Terpyridine -Terpyridine and Higher Oligopyridines, Vol. 30*, Academic Press, **1986**.

[24] a) P. Pechy, F. P. Rotzinger, M. K. Nazeeruddin, O. Kohle, S. M. Zakeeruddin, R. Humphry-Baker, M. Graetzel, *J. Chem. Soc., Chem. Commun.* **1995**, 65-66; b) A. M. W. Cargill Thompson, *Coord. Chem. Rev.* **1997**, *160*, 1-52.

[25] H. Hofmeier, U. S. Schubert, *Chem. Soc. Rev.* **2004**, *33*, 373-399.

Entry for the Table of Contents (Please choose one layout)

Layout 1:

SHORT COMMUNICATION

Sensing platform for rapid and sensitive (parts per billion) detection of Fe^{2+}, Fe^{3+}, Ru^{3+}, and Zn^{2+} in aqueous solutions was proposed.

Boolean logic operations were applied to describe the interaction between the ligand (as a logic gate) and four target cations (four logical inputs).

Crystallographically determined structure of $[Fe(terpy\text{-}PO_3Et_2)_2](ClO_4)_2$ complex was presented.

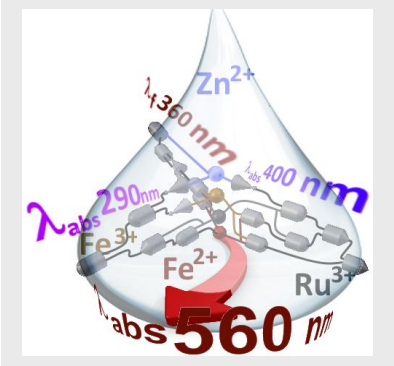

Simultaneous detection*

*Nadia O. Laschuk, Iraklii I. Ebralidze, Denis Spasyuk, and Olena V. Zenkina**

Page No. – Page No.

Multi-readout logic gate for selective metal ions detection in parts per billion levels

*one or two words that highlight the emphasis of the paper or the field of the study